

# Stability of Cu(II)- and Fe(III)-Porphyrins on Montmorillonite Clay: An X-ray Absorption Study

K. A. Carrado\* and S. R. Wasserman\*

Chemistry Division 200, Argonne National Laboratory, Argonne, Illinois 60439

Received July 18, 1995. Revised Manuscript Received September 25, 1995<sup>8</sup>

The Cu(II) and Fe(III) complexes of water-soluble tetrakis(*N,N,N*-trimethylanilinium)-porphyrin (TTAP) and tetrakis(*N*-methylpyridyl)porphyrin (TPyP) were placed within the interlayers of Ca(II)-montmorillonite through ion exchange. The free base forms of the porphyrins were also added to samples of Cu(II)- and Fe(III)-montmorillonites. X-ray absorption spectroscopy (XAS), both X-ray absorption near-edge structure (XANES) and extended X-ray absorption fine structure (EXAFS), were used to monitor the fate of the metal ions. The Cu(II)-metalloporphyrins do not demetalate upon contact with the acidic montmorillonite support. The XAS data also suggest that Fe(III)-porphyrin complexes are stable on smectite supports. XANES data demonstrate that the free base porphyrin TTAP metalates on the surface of a Cu(II)-exchanged clay to form a stable Cu(II)-porphyrin-clay complex.

## Introduction

Metalloporphyrins are important biological materials that form the core of a variety of *in vivo* enzymatic systems for electron transfer.<sup>1</sup> Because of their innate ability to reversibly accept and donate electrons, these compounds are also being developed as catalysts for electrochemical applications<sup>2</sup> and for preparative oxidations of organic compounds.<sup>3</sup> Both homogeneous<sup>4</sup> and heterogeneous versions of catalytic metalloporphyrins have been created. The latter provide enhanced activity and selectivity, as well as facilitating the recovery of the catalyst once the reaction is complete. Organic polymers,<sup>5</sup> and amorphous and crystalline inorganic materials such as silica,<sup>3c</sup> titania,<sup>6</sup> and zeolites<sup>7</sup> have been utilized for the immobilization of these organometallic catalysts. The elucidation of the effect of the support on the catalytic activity of heterogeneous metalloporphyrins and phthalocyanines is an important facet of investigations involving these materials.

In this paper we describe the interaction between metalloporphyrins and smectite clays. Clays offer an inexpensive alternative to zeolites as a catalytic support. Although both clays and zeolites are aluminosilicates in their most typical compositional forms, these two

classes of materials differ in their three dimensional structure and surface acidity.<sup>8</sup> As a result, clays may provide improved stability and enhanced reactivity for metalloporphyrins. In the only previous reports describing the immobilization of metalloporphyrins on smectite clays,<sup>9</sup> linear alkane hydroxylations by Mn-porphyrins were found to be more efficient on montmorillonite clays than with the corresponding homogeneous or silica-supported catalysts.

Smectite clay minerals consist of microcrystalline, layered sheets of aluminosilicates that are negatively charged.<sup>8</sup> These sheets are separated by an interlayer or gallery that contains water and exchangeable cations. The surface acidity of clays such as montmorillonite is composed of both Brönsted and Lewis acid sites. Since the demetalation of metalloporphyrins is highly dependent upon pH,<sup>10</sup> it is critical to determine the extent to which the surface acidity of a support affects the stability of a metalloporphyrin complex. Previous studies have found that several metallocetraphenylporphyrins demetalate on clay surfaces.<sup>11,12</sup> On the other hand, several water-soluble metalloporphyrins are stable to demetalation on clays.<sup>9,13,14</sup>

In this investigation, the metalation-demetalation behavior of two water-soluble porphyrins supported on clays is examined using X-ray absorption spectroscopy (XAS). Each element has a specific X-ray absorption edge, which is, in general, well-differentiated from those of other elements.<sup>15</sup> XAS is therefore an excellent in

<sup>8</sup> Abstract published in *Advance ACS Abstracts*, November 1, 1995.

(1) Fuhrhop, J.-H. *Porphyrins and Metalloporphyrins*; Smith, K. M., Ed.; Elsevier: Amsterdam, 1975; p 593.

(2) (a) Shi, C.; Anson, F. C. *J. Am. Chem. Soc.* **1991**, *113*, 9564. (b) Koval, C. A.; Drew, S. M.; Noble, R. D.; Yu, J. *Inorg. Chem.* **1990**, *29*, 4708. (c) Sazou, D.; Araullo-McAdams, C.; Han, B. C.; Franzen, M. M.; Kadish, K. M. *J. Am. Chem. Soc.* **1990**, *112*, 7879.

(3) (a) Leung, T. W.; Dombek, B. D. *J. Chem. Soc., Chem. Commun.* **1992**, 205. (b) Chiang, L.; Konishi, K.; Aida, T.; Inoue, S. *J. Chem. Soc., Chem. Commun.* **1992**, 254. (c) Battioni, P.; Lallier, J. P.; Barloy, L.; Mansuy, D. *J. Chem. Soc., Chem. Commun.* **1989**, 1149. (d) Herron, N. *J. Coord. Chem.* **1988**, *19*, 25.

(4) Mansuy, D. *Pure Appl. Chem.* **1987**, *59*, 579.

(5) Anson, F. C.; Ni, C.; Saveant, J. *J. Am. Chem. Soc.* **1985**, *107*, 3442.

(6) Fujitsu, H.; Sakakihara, T.; Mochida, I. *Chem. Lett.* **1991**, 159.

(7) (a) Persaud, L.; Bard, A. J.; Campion, A.; Fox, M. A.; Mallouk, T. E.; Webber, S. E.; White, J. M. *J. Am. Chem. Soc.* **1987**, *109*, 7309. (b) Li, Z.; Wang, C. M.; Persaud, L.; Mallouk, T. E. *J. Phys. Chem.* **1988**, *92*, 2592. (c) deVismes, B.; Bedioui, F.; Devynck, J.; Bied-Charetton, C.; Peree-Fauvet, M. *Nouv. J. Chim.* **1986**, *10*, 81.

(8) Barrer, R. M. *Zeolites and Clay Minerals as Sorbents and Molecular Sieves*; Academic Press: New York, 1978.

(9) (a) Barloy, L.; Battioni, P.; Mansuy, D. *J. Chem. Soc., Chem. Commun.* **1990**, 1365. (b) Battioni, P.; Barloy, L.; Mansuy, D.; Palvadeau, P.; Tournoux, M.; Piffard, Y.; Rouxel, J. *Pillared Layered Structures: Current Trends and Applications*; Mitchell, I. V., Ed.; Elsevier: Amsterdam, 1990; pp 195-197.

(10) Buchler, J. W. *Porphyrins and Metalloporphyrins*; Smith, K. M., Ed.; Elsevier: Amsterdam, 1975; pp 195-199.

(11) Van Damme, H.; Crespin, M.; Obrecht, F.; Cruz, M. I.; Fripiat, J. *J. Colloid Interface Sci.* **1978**, *66*, 43.

(12) Bergaya, F.; Van Damme, H. *Geochim. Cosmochim. Acta* **1982**, *46*, 349.

(13) Carrado, K. A.; Winans, R. E. *Chem. Mater.* **1990**, *2*, 328.

(14) Giannelis, E. P. *Chem. Mater.* **1990**, *2*, 627.

situ probe of both the structural and electronic environment of a metal atom. This technique has been used in the past to examine transition metals within the crystalline, layered framework lattices of clays.<sup>16</sup> The structure of ions within the less-ordered interlayers of clays, including uranyl,<sup>17</sup> lanthanides,<sup>18</sup> chromium,<sup>19</sup> and cobalt,<sup>20</sup> have also been the subject of XAS experiments. Recently, the coordination changes encountered by a solvated solid-state copper(II) cation as it dissolved in excess solvent within the layers of a montmorillonite were reported.<sup>21</sup> XAS studies of homogeneous metalloporphyrins have also been quite extensive. The spectra for complexes of porphyrins with iron(II) and iron(III),<sup>22</sup> as well as several other metals,<sup>23</sup> have been reported.

The employment of XAS for such studies offers more than the advantage of element specificity. This technique permits the direct observation of both the chemical state and coordination structure of the metal ion under investigation. Alternative methods, such as UV-visible absorption,<sup>24</sup> diffuse reflectance UV-visible absorption,<sup>13,25</sup> and X-ray photoelectron (XPS) spectroscopies,<sup>25b</sup> often offer only an indirect probe for the metal ion. For example, in previous studies of the metalation-demetalation behavior of porphyrins on supports such as zeolites,<sup>26</sup> graphite,<sup>24</sup> and smectite clays,<sup>25</sup> the state of the metal ion was deduced through shifts in the N<sub>1s</sub> binding energies (XPS) or changes in the Soret bands from the porphyrin in the absorption spectrum of the complex (UV-vis).

In this study, water-soluble free base tetrakis(*N*-methylpyridyl)porphyrin (TMPyP) and tetrakis(*N,N,N*,

(15) (a) Sayers, D. E.; Bunker, B. A. In *X-Ray Absorption: Principles, Applications, Techniques of EXAFS, SEXAFS, and XANES*; Koningsberger, D. C., Prins, R., Eds.; John Wiley & Sons: New York, 1988; Chapter 6. (b) Teo, B. K. *EXAFS: Basic Principles and Data Analysis*; Springer-Verlag: Berlin, 1986.

(16) (a) Stouff, P.; Boulegue, J. *Am. Mineral.* **1988**, *73*, 1162. (b) Manceau, A.; Calas, G. *Clay Miner.* **1986**, *21*, 341. (c) Manceau, A.; Bonnin, D.; Stone, W. E. E.; Sanz, J. *Phys. Chem. Miner.* **1990**, *17*, 363.

(17) Dent, A. J.; Ramsay, J. D. F.; Swanton, S. W. *J. Colloid Interface Sci.* **1992**, *150*, 45.

(18) Jones, D. J.; Roziere, J.; Olivera-Pastor, P.; Rodriguez-Castellon, E.; Jimenez-Lopez, A. *J. Chem. Soc., Faraday Trans.* **1991**, *87*, 3077.

(19) Bornholdt, K.; Corker, J. M.; Evans, J.; Rummey, J. M. *Inorg. Chem.* **1991**, *30*, 1.

(20) Fukushima, Y.; Okamoto, T. *Proc. Inter. Clay Conf., Denver 1985*; Schultz, L. G., van Olphen, H., Mumpton, F. A., Eds.; The Clay Minerals Society: Bloomington, IN, 1987; p 9.

(21) Carrado, K. A.; Wasserman, S. R. *J. Am. Chem. Soc.* **1993**, *115*, 3394.

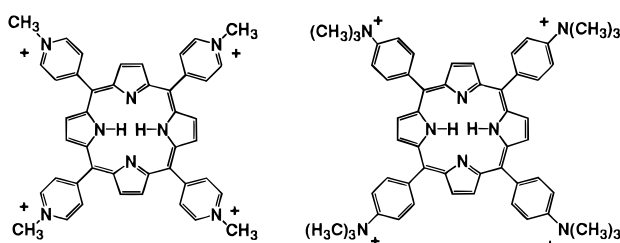
(22) (a) Cartier, C.; Momenteau, M.; Dartige, E.; Fontaine, A.; Tourillon, G.; Michalowicz, A.; Verdaguer, M. *J. Chem. Soc., Dalton Trans.* **1992**, *609*. (b) Kim, S.; Bae, I. T.; Sandifer, M.; Ross, P. N.; Carr, R.; Woicik, J. A.; Antonio, M.; Scherson, D. A. *J. Am. Chem. Soc.* **1991**, *113*, 9063. (c) Wang, S.; Waldo, G. S.; Fronko, R.; Penner-Hahn, J. E. *Physica B* **1989**, *158*, 119. (d) Kau, L.-S.; Svasstis, E. W.; Dawson, J. H.; Hodgson, K. O. *Inorg. Chem.* **1986**, *25*, 4307.

(23) (a) Tabata, M.; Ozutsumi, K. *Bull. Chem. Soc. Jpn.* **1992**, *65*, 1438. (b) Kajiwara, A.; Kamachi, M.; Maeda, H. *Polym. J.* **1991**, *23*, 343. (c) Furenlid, L. R.; Renner, M. W.; Smith, K. M.; Fajer, J. J. *Am. Chem. Soc.* **1990**, *112*, 1634. (d) Ruiz-Lopez, M. F.; Natoli, C. R. *J. Chim. Phys. Phys.-Chim. Biol.* **1989**, *86*, 905. (e) Asahina, H.; Zisk, M. B.; Hedman, B.; McDevitt, J. T.; Collman, J. P.; Hodgson, K. O. *J. Chem. Soc., Chem. Commun.* **1989**, 1360. (f) Goulon, J.; Friant, P.; Goulon-Ginet, C.; Coutsolelos, A.; Guilard, R. *Chem. Phys.* **1984**, *83*, 367.

(24) Lipiner, G.; Willner, I.; Aizenshtat, Z. *J. Chem. Soc., Chem. Commun.* **1987**, 34.

(25) (a) Abdo, S.; Cruz, M. I.; Fripiat, J. J. *Clays Clay Miner.* **1980**, *28*, 125. (b) Canesson, P.; Cruz, M. I.; van Damme, H. *Inter. Clay Conf., Mortland*, M. M., Farmer, V. C., Eds.; Elsevier: Amsterdam, 1978; p 217.

(26) Roth, S. A.; Iton, L. E.; Fleisch, T. H.; Meyers, B. L.; Marshall, C. L.; Delgass, W. N. *J. Catal.* **1987**, *108*, 214.



TMPyP

TTAP

**Figure 1.** Water-soluble meso-substituted porphyrins tetrakis(*N*-methylpyridyl)porphyrin (TMPyP) and tetrakis(trimethyl anilinium) porphyrin (TTAP).

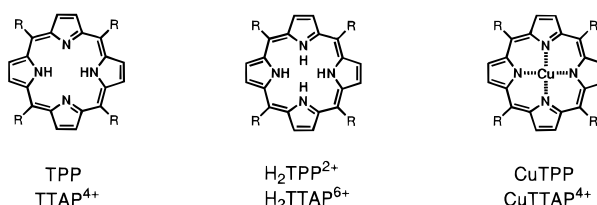


**Figure 2.** Various charges and complexes of tetraphenylporphyrin (TPP, R = phenyl) and tetrakis(trimethyl anilinium)-porphyrin (TTAP<sup>4+</sup>, R = trimethylanilinium): as the free bases on the left, as the cations in the center, and as the copper complexes on the right.

trimethylanilinium)porphyrin (TTAP), and their copper(II) and iron(III) metallo analogues were loaded onto a montmorillonite clay. Figure 1 shows the structures of these molecules. Each of these compounds has four quaternary nitrogen groups on the exterior of the porphyrin. The resulting positive charge enhances the solubility of these compounds in water and their affinity for the negatively charged lattice of the clay. Figure 2 illustrates the various complexes of TTAP and compares the total charge of these compounds to that found with the analogous metallo complexes of water-insoluble tetraphenylporphyrin (TPP). We also attempted to create supported metalloporphyrins by sequential addition of metal ions and free base porphyrins to montmorillonite. XAS, including both the X-ray absorption near edge structure (XANES) and the extended X-ray absorption fine structure (EXAFS), were used to monitor the fate of the metal ions. The results of X-ray diffraction, as well as those from earlier UV-visible experiments,<sup>11</sup> were also used to aid in deducing the structure of the metal-porphyrin-clay systems.

## Experimental Section

Samples were prepared as previously reported.<sup>13</sup> The chloride salts of water-soluble TMPyP, TTAP, and their copper(II) and iron(III) metallo analogues were used as purchased from Midcentury Chemicals, Ltd., Posen, IL. Bentolite L, a Ca(II)-montmorillonite from which all but 0.3 wt % iron oxides have been removed, was obtained from Southern Clay Products, Gonzales, TX. The Ca(II) ions within the interlayers of the clay were replaced by Cu(II), Fe(III), porphyrin, or metalloporphyrin ions by routine ion-exchange methods. The clay (0.25 g) was stirred as a slurry in the aqueous porphyrin solution (50 mL,  $1 \times 10^{-3}$  M) for 24 h, then isolated, thoroughly washed, and air-dried. Samples for which the metalloporphyrin was added directly to the clay are designated as CuTTAP-clay. TTAP/Cu-clay denotes a sample resulting from the addition of free base porphyrin ions to clays which already contain transition-metal cations (Fe-clay or Cu-clay).

The lattice spacings (001) for each of the clays were monitored using X-ray powder diffraction. The diffraction

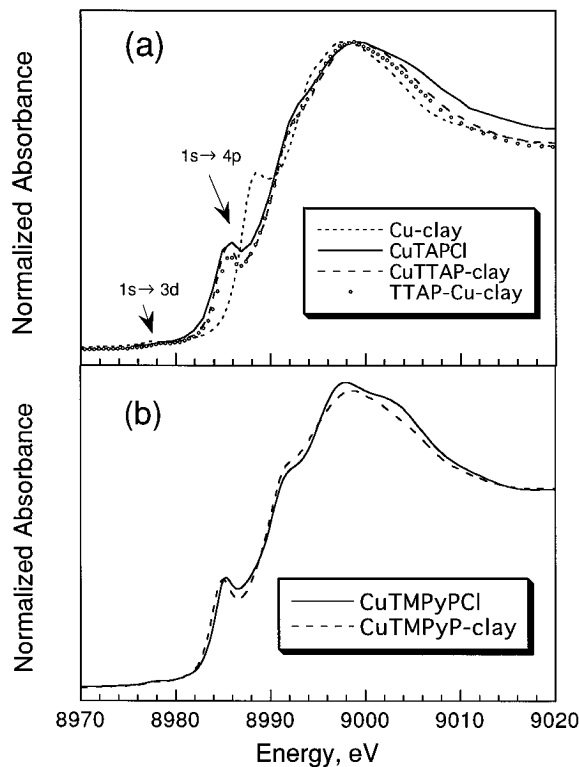


**Figure 3.** Normalized Cu(II) K-edge absorption spectra. All are fluorescence spectra except CuTAPCl and CuTMPyPCl, which are transmission spectra.

patterns were obtained on a Scintag PAD V instrument with Cu K $\alpha$  radiation.

Transmission and fluorescence copper and iron K-edge X-ray absorption spectra were acquired at the National Synchrotron Light Source at Brookhaven National Laboratory on beamlines X23A2 and X19A, and at station IV-3 of the Stanford Synchrotron Radiation Laboratory in Stanford, CA. The latter two beamlines were equipped with Si[220] double-crystal monochromators. A Si[311] double crystal monochromator was used at X23A2. Harmonics from the Si[220] monochromators were rejected by detuning the crystals to approximately 50% of their maximum transmission. Standard ion chambers, filled with nitrogen gas, were used to monitor the incoming and transmitted X-ray beams for each of the samples. A Lytle detector, with argon in the ionization chamber, was utilized for the fluorescence data. The energy calibration was maintained by simultaneously monitoring the maxima in the derivative spectra of the respective metal foils. The precision of the energy calibration is 0.3 eV. The reported data are the average of two or three scans. Standard methods were used for the analysis of the XANES and EXAFS spectra.<sup>15</sup> XAMath, an XAS analysis package based on Mathematica developed at Argonne National Laboratory, was used for the reduction of the original data.

## Results and Discussion

**Cu(II) Samples.** Figure 3 shows the normalized fluorescence X-ray absorption near edge (XANES) spectra for the copper(II) ion in Cu-clay, CuTTAP-clay, and sequentially exchanged TTAP/Cu-clay, as well as the transmission spectrum for pure CuTTAPCl. These samples provide two windows through which to examine the metalation–demetalation behavior of copper and porphyrins within a clay. The CuTTAP-clay sample is monitored to determine if the Cu(II)–porphyrin complex is stable to demetalation when placed inside the interlayer of a clay. The sequentially exchanged sample probes whether or not free-base porphyrin

metalation takes place within the galleries of a clay that already contains free metal ions.

X-ray absorption spectroscopy is particularly useful for monitoring the association of copper ions with porphyrins. The onset of the copper edge typically shifts to higher energies with increasing formal oxidation state: 3–4 eV from Cu(I) to Cu(II), and approximately 2 eV from Cu(II) to Cu(III).<sup>27</sup> These values assume that the type of ligands surrounding the copper atom are similar in each case. In general, the location of an absorption edge is dependent on the electron donating ability of the ligands associated with the absorbing atom, even for systems which nominally have the same formal oxidation state. Since in the case of metalation within a clay, the nitrogen-based porphyrin replaces the water ligands in the first coordination sphere of the copper atom, XAS provides a direct method for monitoring this exchange.

Normally it is difficult to separate the contributions to the location of the X-ray edge of formal oxidation state and the electron donating ability of the ligand. In the case of copper, however, this difficulty is minimized. The +2 oxidation state of copper is indicated by the occurrence of the weak 1s → 3d transition at 8977 eV. This transition cannot occur for Cu(I) because all the d orbitals are filled (3d<sup>10</sup>). As long as this transition appears in the XANES spectrum, the copper is formally in the +2 (or higher) oxidation state. Although the 1s → 3d transition does appear for Cu(II), it is of low intensity because it is forbidden in the dipolar approximation ( $\Delta J \neq 1$ ).<sup>28</sup>

Each of the spectra in Figure 3 clearly display the electronic 1s → 4p transition as a resolved shoulder on the Cu(II) absorption edge. This transition, which is characteristic of a copper ion with square-planar coordination,<sup>28</sup> occurs at 8989 eV for the copper ion complexed with water.<sup>29</sup> The shoulder appears at lower energy, 8986 eV, for each of the porphyrin complexes. While square-planar copper(II) in a porphyrin is expected, the fact that this geometry appears in the Cu-clay indicates that the ion exists in this particular hydrated sample as Cu(H<sub>2</sub>O)<sub>4</sub><sup>2+</sup>. When more water is present within the clay, this transition can broaden and disappear, although the position of the overall edge, as monitored by the derivative, does not change appreciably.<sup>21</sup> Despite the appearance of the edge at lower energy for the CuTTAP materials, the weak 1s → 3d transition is present for each of the copper–porphyrin complexes. The appearance of this transition confirms that the copper ions associated with the porphyrins are still in the +2 oxidation state. Therefore, the shift in energy of the absorption edge for the metalloporphyrin reflects the difference in coordination by oxygen and nitrogen atoms. The edge occurs at lower energy because of the greater electron-donating ability of the nitrogen atoms in the macrocycle.

The Cu(II) K edges, including the 1s → 4p transitions, for the three copper(II) porphyrin samples (CuTTAPCl,

(27) Soderholm, L.; Goodman, G. L. *J. Opt. Soc. Am. B* **1989**, 6, 483.

(28) Lytle, F. W.; Greggor, R. B.; Panson, A. J. *Phys. Rev. B* **1988**, 37, 1550.

(29) (a) Kau, L.-S.; Spira-Solomon, D. J.; Penner-Hahn, J. E.; Hodgson, K. O.; Solomon, E. I. *J. Am. Chem. Soc.* **1987**, 109, 6433. (b) Alp, E. E.; Shenoy, G. K.; Hicks, D. G.; Capone II, D. W.; Soderholm, L.; Schuttler, H. B.; Guo, J.; Ellis, D. E.; Montano, P. A.; Ramanathan, M. *Phys. Rev. B* **1987**, 35, 7199.

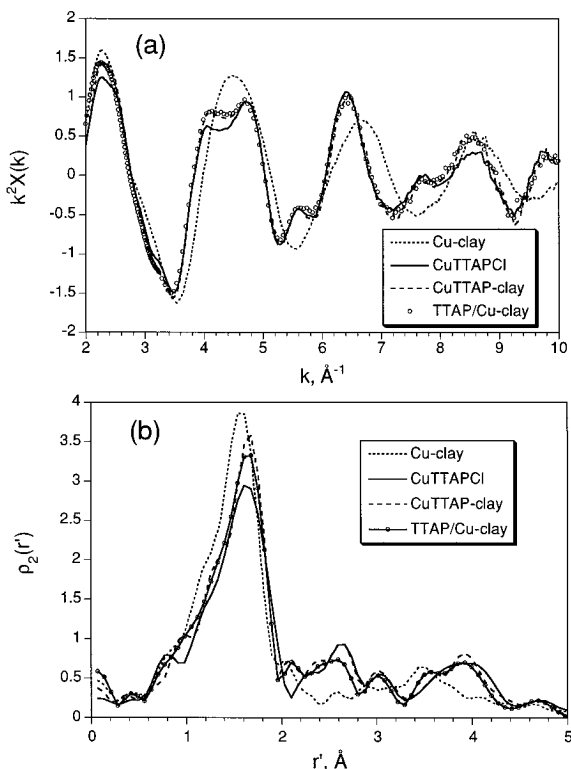


**Figure 4.** (a) Unfiltered  $k^2$ -weighted EXAFS,  $k^2\chi(k)$ , and (b) radial structure functions ( $\Delta k = 1.8\text{--}13\text{ }\text{\AA}^{-1}$ ).

CuTTAP-clay, and TTAP/Cu-clay are virtually identical (Figure 3a). Two important conclusions can be drawn from this observation. First, incorporation of CuTTAP by the montmorillonite to form CuTTAP-clay does not result in demetalation of the ion from the porphyrin. The metalloporphyrin remains intact within the clay galleries. Second, ion exchange of a free base porphyrin into Cu-clay (TTAP/Cu-clay) results in a species which is chemically identical to that created when the preformed metalloporphyrin is introduced into the clay. Within the environment of the clay galleries, complexation of a metal ion and a porphyrin can occur. The stability of the copper-porphyrin complex has been confirmed with another water-soluble porphyrin, TMPyP. The XANES spectra for CuTMPyP-clay and CuTMPyPCl are virtually identical to those of the corresponding TTAP systems (Figure 3b).

The radial structure functions, which are deduced from the EXAFS signal above the absorption edge, also indicate the association of the Cu ion with the porphyrin. Figure 4 shows the  $k^2$ -weighted EXAFS spectra and the corresponding radial distributions of the four samples whose near-edge spectra are presented in Figure 3a. The spectra for the three porphyrin samples are similar. As is true for the XANES spectra, the hydrated copper in Cu-clay is distinct from that of the metalloporphyrins. The radial structure functions of the Cu-porphyrins have significant features at distances greater than 2 Å which are not found in the Cu-clay sample. These peaks reflect the greater short-range (2–5 Å) order of the porphyrin-containing clays, in which the copper(II) cation is held within the macrocycle. Table 1 lists the fitting parameters for the first coordination shell of each of the Cu-porphyrin samples. The coordination numbers and the bond distances are, to within the standard errors for EXAFS analysis,<sup>15</sup> the same for each sample.

**Table 1. Parameters for the First Coordination Shell in the EXAFS Spectra of Cu-porphyrins<sup>a</sup>**

sample	$n$	$r$	$10^3\Delta\sigma^2$	$\Delta E$
CuTTAPCl	4	1.98	0	0
CuTTAP-clay	3.9	1.97	-3	-0.6
TTAP/Cu-clay	4.1	1.97	-1	-1.2
CuTMPyPCl	4.2	1.97	-0.9	-0.1
CuTMPyP-clay	3.9	1.98	-3	0

<sup>a</sup> The estimated errors in coordination number ( $n$ ) and radial distance ( $r$ ) are  $\pm 10\%$  of  $n$  and  $\pm 0.01\text{ }\text{\AA}$ , respectively. The values for  $n$ ,  $r$ ,  $\Delta\sigma^2$ , and  $\Delta E$  are referred to the spectrum of pure CuTTAPCl ( $n = 4$ ,  $r = 1.98$ ,  $\Delta\sigma^2 = 0$ ,  $\Delta E = 0$ ). The length of the Cu–N bond in the reference, 1.98 Å, was assumed to be the same as that in Cu-tetraphenylporphyrin.<sup>34</sup> The windows for the forward and reverse Fourier transforms were  $\Delta k = 1.8\text{--}13\text{ }\text{\AA}^{-1}$  and  $\Delta r = 0.8\text{--}1.97\text{ }\text{\AA}$  respectively. The  $k^2$ -weighted EXAFS data,  $k^2\chi(k)$ , were modeled in the range  $\Delta k = 2\text{--}12\text{ }\text{\AA}^{-1}$ .

**Table 2. Interlayer (001) Spacings from X-ray Diffraction**

sample	$d(001)$ , Å	sample	$d(001)$ , Å
Cu-clay	12.4	TMPyP/Cu-clay	14.3
TTAP-clay <sup>a</sup>	15.2	Fe-clay	12.8
TMPyP-clay <sup>a</sup>	15.0	FeTTAP-clay	18.0
CuTTAP-clay	18.0	TTAP/Fe-clay	14.7
TTAP/Cu-clay	15.2, 18.0	FeTMPyP-clay	16.7
CuTMPyP-clay	14.0 <sup>b</sup>	TMPyP/Fe-clay	13.9

<sup>a</sup> Clay = STx-1, a  $\text{Ca}^{2+}$ -montmorillonite from Texas. <sup>b</sup> Reference 14.

The conclusions that copper-porphyrins are stable inside a clay and that, within this environment, metalation can proceed as in solution, agree with results obtained earlier from diffuse reflectance UV-visible absorption spectroscopy (DRS).<sup>13</sup> Only the XAS measurements, however, provide a quantitative assessment of the degree to which the Cu(II) ion has reacted with the porphyrin. In the DRS experiments, the changes in the characteristic absorption bands upon metalation or demetalation are quite significant. But, since the UV-visible spectrum of the  $\text{Cu}(\text{H}_2\text{O})_4^{2+}$  complex is much less intense than that of the porphyrins, it is not possible to determine how much hydrated metal remains after addition of the free-base porphyrin. The X-ray absorption edge spectra indicate that after exposure of Cu-clay to the water-soluble TTAP, most if not all of the Cu(II) ions within the clay are complexed to the pyrrolic nitrogens of the porphyrin. Inspection of the first derivatives of the edges fails to find the signature of the  $1s \rightarrow 4p$  transition of the aquo-copper species. We have also performed a nonlinear least-squares fit of the absorption edge of TTAP/Cu-clay using CuTTAP-clay and Cu-clay as the reference edges. This alternative analysis suggests that at least 80% of the Cu in TTAP/Cu-clay is present as the metalloporphyrin.

Other experimental methods provide confirmation for these conclusions. The DRS experiments suggest that TTAP metalates on a Cu-clay surface, and that CuTTAP remains intact when introduced into the clay.<sup>13</sup> The UV-visible measurements also indicate that some unassociated porphyrin is retained in the interlayer of the Cu-clay. The X-ray diffraction patterns from the clays (Table 2) demonstrate that the basal spacings,  $d(001)$ , of both Cu-TTAP/clay samples are similar at 18.0 Å. This number is considerably greater than the 12.4 Å observed for Cu-clay. The TTAP/Cu-clay sample also shows an additional, weak (001) spacing of 15.2 Å. This lattice parameter, which is similar to that

of unmetallated TTAP-clay<sup>13</sup> (15.7 Å) probably indicates the presence of the unmetallated porphyrin within the interlayer. Therefore, TTAP/Cu-clay has the great majority of Cu tied up as a metalloporphyrin. The interlayer of this material also contains some uncomplexed free base porphyrin molecules. The amount of copper that remains as hydrated ions is, if any, small.

The basal spacings for the Cu-TMPyP samples are lower than those of the corresponding TTAP complexes (14.0 Å for CuTMPyP-clay and 14.3 Å for TMPyP/Cu-clay vs 18.0 Å for both CuTTAP-clay and TTAP/Cu-clay). Despite the differences in the lattice spacings, the XAS spectra demonstrate that the copper environments in the CuTMPyP-clay and CuTTAP-clay are similar. The larger (001) spacings for the TTAP materials have been attributed to an increased tilting of this macrocycle within the clay galleries.<sup>13,14</sup> Together, the XAS and diffraction data imply that while the metal coordination is similar in the two porphyrins, the orientations of the metal-organic complexes within the interlayer of the clay are quite different.

Previous work with water-insoluble Cu(II) porphyrins found that when the free-base tetraphenylporphyrin (TPP) is adsorbed by a Cu-clay, only a small amount of the macrocycle enters the clay gallery. The porphyrin taken up by the clay does not associate with the metal ion, but instead remains as the dication.<sup>11</sup> Upon addition of tetrapyridyl porphyrin (TPyP) to Cu-clay, however, the characteristic visible spectrum of the Cu(II)TPyP complex is observed.<sup>11</sup> Our observation of metalation to form Cu(II)TTAP and Cu(II)TMPyP is consistent with this latter work. The difference in behavior between water-soluble and water insoluble porphyrins is due to their differences in charge density. TMPyP and TTAP each have four positive charges from the peripheral pyridinium or anilinium groups (see Figure 1). The presence of these charges increases the affinity of the porphyrin for the hydrophilic environment of the clay galleries. Furthermore, the peripheral quaternary nitrogens provide an electrostatic interaction with the negative charges localized within the octahedral sites of the aluminosilicate lattice. These cationic sites are absent in neutral macrocycles such as TPP. To gain electrostatic attraction to the clay, these neutral molecules protonate the pyrrolic nitrogen atoms. Incorporation of Cu(II) inside the heme group prevents this protonation and eliminates the driving force for interaction with the clay surface. The peripheral nitrogen atoms on TPyP can protonate, generating a positively charged complex in which the pyrrolic macrocycle is free to incorporate Cu(II).

**Fe(III) Samples.** Figure 5a shows the XANES spectra from four iron(III) samples: the fluorescence spectra of Fe-clay, FeTTAP-clay, and sequentially exchanged TTAP/Fe-clay, and the transmission spectrum from pure FeTTAPCl. These four samples are analogous to those for copper discussed above. The four iron edges do not, however, exhibit the same trends that were discerned in the copper systems. Each of the copper-porphyrin complexes were similar and clearly differentiated from Cu-clay. In contrast, the spectra from Fe-clay, FeTTAP-clay, and TTAP/Fe-clay are similar. The onset of each of these edges at approximately 7112 eV is typical of iron in the +3 oxidation state.<sup>22</sup> The XAS spectrum from the pure

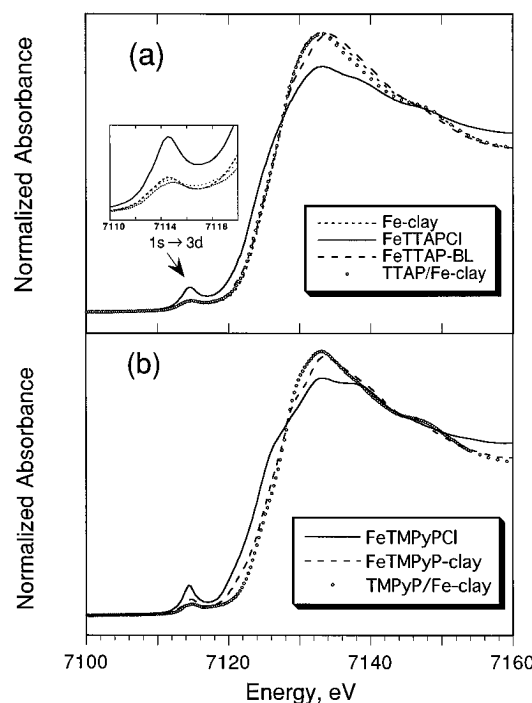


**Figure 5.** Normalized Fe(III) K-edge absorption spectra. All are fluorescence spectra except FeTTAPCl, which is a transmission spectrum.

iron(III) porphyrin chloride salt does not match that of the other iron-porphyrin systems. As was found for the copper systems, changing the peripheral groups in the porphyrin does not affect the spectra. The X-ray absorption spectra for FeTMPyPCI, FeTMPyP-clay, and TMPyP/Fe-clay are similar to those of the corresponding FeTTAP systems (Figure 5b),<sup>30</sup> although the edges of the two TMPyP clay samples exhibit somewhat greater differences than were found for the TTAP/Fe- and FeTTAP-clays.

The small preedge feature near 7115 eV is, as is the feature at 8979 in the Cu(II) spectra, a transition of the photoelectron from the 1s level of the iron(III) cation to an excited state involving the 3d orbitals.<sup>22a</sup> The influence of symmetry on the intensity of this feature in the spectra of Fe-porphyrins has been demonstrated by others.<sup>31</sup> The intensity increases as the coordination symmetry changes from square planar to octahedral to square pyramidal.<sup>22a</sup> This variation in intensity reflects a change in the degree to which the 4p and 3d orbitals of the ferric ion interact. Within the four Fe-clay samples, the preedge transition is of greatest intensity for FeTTAPCl. In this sample, the geometry around Fe(III) is presumably square pyramidal. This configuration arises from the requirement of charge neutrality. The planar pyrrolic macrocycle, which is neutral prior to interaction with the metal, loses two protons during metalation, resulting in a formal -2 charge. To compensate for the remainder of the +3 charge from the iron cation in FeTTAPCl, the chloride ion serves as the

(30) Due to experimental difficulties, Figures 5–7 include data from the fluorescence spectrum of pure FeTMPyPCI. On the basis of a comparison of the fluorescence and transmission spectra of FeTTAPCl, we conclude that, in the fluorescence spectra, self-absorption effects result in a reduction of the intensity of the EXAFS signal by approximately 20%. This decrease in intensity does not affect the conclusions presented here.

(31) Roe, A. L.; Schneider, D. J.; Mayer, R. J.; Pyrz, J. W.; Windom, J.; Que, L. *J. Am. Chem. Soc.* **1984**, *106*, 1676.

fifth ligand to the central atom in the pure Fe-porphyrin.

The  $1s \rightarrow 3d$  feature is less intense for the remaining three Fe samples, suggesting either square planar or octahedral coordination. Generally, Fe(III) coordination complexes prefer octahedral coordination.<sup>32</sup> Indeed, previous XAS studies of iron porphyrins have found that square planar coordination is possible only in an Fe(II) basket-handle porphyrin.<sup>22a</sup> In this case, where the metal atom is shielded from further ligation by the long chain alkyl groups on the porphyrin, the  $1s \rightarrow 4p$  transition appears. The  $1s \rightarrow 4p$  transition is not present in the absorption edges presented here, a fact confirmed by examination of the first derivative of the spectra. We therefore deduce that the Fe-clay, Fe-TTAP-clay, and TTAP/Fe-clay samples all have iron in an octahedral environment. In these systems, the charge balance is maintained through the negative charge within the aluminosilicate lattice of the clay, rather than by a chloride ion bound directly to the Fe(III) cation.

The spectra from FeTTAP-clay and TTAP/Fe-clay appear to imply that the iron in these two systems are similar. Related studies based on diffuse reflectance data have reached conflicting conclusions concerning the stability of Fe(III) metalloporphyrins on clay surfaces. One investigation concluded that an Fe(III) porphyrin is irreversibly demetalated and protonated,<sup>11</sup> while two others found that a Fe(III) porphyrin is the stable adsorbed complex on montmorillonite and hectorite clays.<sup>12,13</sup> These experiments also suggested that, in contrast to the Cu(II) systems, iron and porphyrin would not combine within the gallery of the clay.<sup>13</sup> X-ray powder diffraction experiments intimate that addition of Fe and porphyrin in sequence does not result in the same product as does direct incorporation of a metalloporphyrin. The (001) lattice spacing of the FeTTAP-clay is 18 Å, while that for TTAP/Fe-clay is 14.7 Å. A similar change (16.7 Å for FeTMPyP-clay vs 13.9 Å for TMPyP/Fe-clay) is observed with the pyridinium porphyrin. These spacings are greater than that in Fe-clay (12.8 Å). The spacing for TTAP/Fe-clay is similar to that found when this porphyrin is placed within a clay which does not contain iron (15.2 Å). This observation provides confirmation for the DRS results which indicated that the porphyrin and iron do not combine inside the clay.<sup>13</sup> We note that the lattice spacings of the FeTTAP and FeTMPyP clays are greater than that of a clay which contains only the free base porphyrin (TTAP-clay). This result implies that in order to maintain octahedral coordination, the iron in these systems probably have two additional water molecules as ligands. In the Fe-exchanged clay, the small lattice spacing suggests that the axial ligands about the Fe(III) ion may be the clay lattice itself. When the porphyrin is present, it apparently sterically prevents the clay from complexing with the metal at the axial positions.

The question remains of whether the similarity in the XANES spectra of FeTTAP-clay and TTAP/Fe-clay actually demonstrates that the species present in the gallery of the clay are the same in these two samples, a conclusion that would be at variance with the DRS and

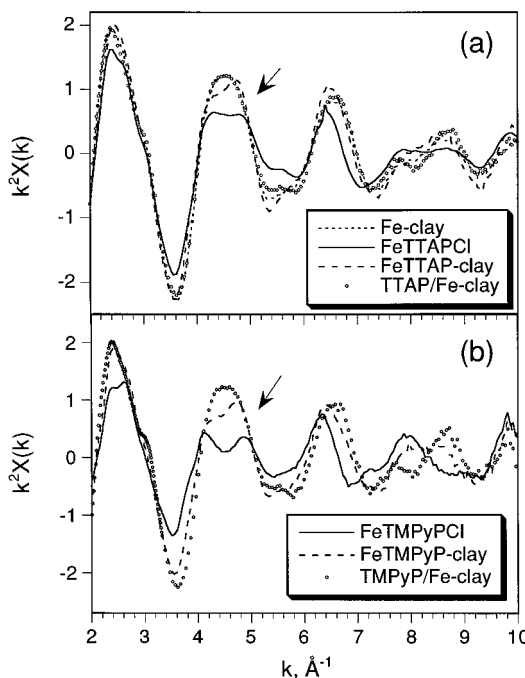


**Figure 6.** Unfiltered,  $k^2$ -weighted EXAFS,  $k^2\chi(k)$ . The arrows indicate the section of the data which differentiates between the aquo-Fe and Fe-porphyrin species.

X-ray diffraction data. In analogy with the copper systems discussed above, one may expect the Fe-porphyrin samples to exhibit a shift to lower energy similar to those observed with the copper-porphyrin systems. The lack of such a shift might indicate that the metalloporphyrin has demetalated, resulting in Fe(III) complexed solely with water. However, the octahedral nature of the iron ions adds an additional complication. The exchange of TTAP or TMPyP for the water molecules bound to copper results in a complete transformation of the ligands on the central atom from oxygen to nitrogen. In contrast, the porphyrin replaces only four of the six moieties around the octahedral iron. The two other species bound to the ferric ion are presumably oxygen, from either water molecules or the basal surface of the clay. Therefore the shift in the absorption edge of Fe(III) as its ligands change from oxygen to nitrogen may not be as large as that observed for copper(II). Indeed, the spectra presented here suggest that the species with mixed ligation have absorption edges similar to that of the completely oxygenated iron found in Fe-clay.

The EXAFS spectra for the various Fe-porphyrins provide the best evidence that the coordination of iron in FeTTAP-clay is, in fact, different from that in TTAP/Fe-clay. The unfiltered,  $k^2$ -weighted spectra for these samples, as well as those for Fe-clay and pure FeTTAPCl, are shown in Figure 6a. The corresponding radial structure functions appear in Figure 7a. Unlike the copper systems, there is not a great change in the phase of the EXAFS data between the Fe-clay and the Fe-porphyrins. Other features of the EXAFS spectra, however, may be used to differentiate between these species. The spectra for TTAP/Fe and Fe-clay are, to within experimental error, the same. This result suggests that the same local coordination for iron is found in these two materials. Since the Fe-clay only has ligation of the iron by oxygen, we conclude that the cation in the TTAP/Fe-clay has not associated with the

(32) Cotton, F. A.; Wilkinson, G. *Advanced Inorganic Chemistry*, 4th ed., Wiley-Interscience: New York, 1980; p 751.

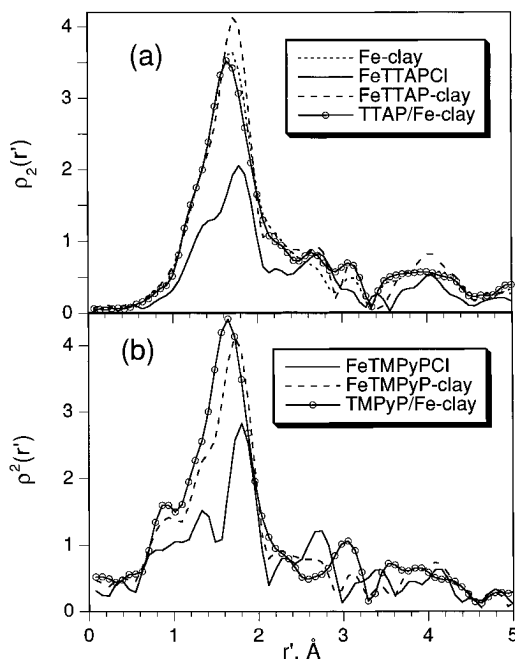


Figure 7. Radial structure functions ( $\Delta k = 2-12 \text{ \AA}^{-1}$ ).

porphyrin. It is instead present as an aquo species as is found in the Fe-clay. On the other hand, the EXAFS spectra for FeTTAP-clay and FeTTAPCI are distinct from one another and those of the other two samples. In particular, the maximum in the EXAFS oscillations at  $k = 4.5 \text{ \AA}^{-1}$  has a different shape from that observed for TTAP/Fe- and Fe-clay. The same general behavior is found with the analogous TMPyP clays (Figures 6b and 7b). The lower amplitude of the EXAFS in the metalloporphyrin chloride salts reflects the presence of the chloride ion in the coordination sphere of the iron cation. The scattering of X-rays by chlorine is somewhat out of phase to that from the pyrrolic nitrogen atoms and results in a lowering of the intensity of the EXAFS.<sup>33</sup> The shapes of the EXAFS signals from FeTTAP-clay and FeTMPyP-clay are midway between those of the native metalloporphyrin and Fe-clay. We believe that this fact indicates that, at the very least, a significant fraction of the metalloporphyrin remains intact upon addition to the clay.

(33) We have modeled the effect of the chloride ion on the EXAFS signal of metalloporphyrins using FEFF6, an ab initio program for calculating EXAFS spectra. Zabinsky, S. I.; Rehr, J. J.; Ankudinov, A.; Albers, R. C.; Eller, M. J. *Phys. Rev. B* **1995**, *52*, 2995. The spectrum was calculated using the structure for FeTPPOH-H<sub>2</sub>O in ref 33. The hydroxy group was replaced with a chlorine atom whose distance from the central iron atom was 0.3 Å greater than that of the oxygen atom.

(34) Fleischer, E. B.; Miller, C. K.; Webb, L. E. *J. Am. Chem. Soc.* **1964**, *86*, 2342.

Since we find that iron and porphyrin do not associate within the clay, while preformed metalloporphyrins are stable on a clay surface, we conclude that the stability of iron-porphyrins in clays is not merely a function of equilibrium thermodynamics. Other factors, including steric constraints on the association of the iron and the macrocycle within a clay interlayer, play an important role in determining whether the organometallic complex forms. Finally, we note that the near-edge spectra for Fe(III)-porphyrins are not as sensitive a probe for coordination as they are for Cu(II) porphyrins.

## Conclusions

These experiments have examined the complexation chemistry of Cu(II) and Fe(III) with water-soluble porphyrins within the interlayers of smectite clays. The results demonstrate that Cu(II) porphyrins are stable within the slightly acidic clay environment and that Cu(II) ions associate with porphyrins inside clays. Iron(III)-porphyrins are also stable on clay surfaces. Unlike the copper moieties, however, ferric ions and porphyrin do not appear to complex when introduced into a clay sequentially. These results illustrate that the chemistry which occurs within a smectite clay is governed by several factors. Factors that may play an important role include the size of the interlayer, orientation of the porphyrin to the sheets of aluminosilicate, surface acidity, and stability of the metalloporphyrin.

This study has demonstrated the utility of X-ray absorption spectroscopy to probe the chemical environment of metal ions inside clays. XAS can illuminate both the local geometry of the ions and their chemical state. It also provides the ability to directly probe how the coordination of the metal ions changes during chemical modification. Such information is crucial for the development of new catalytic systems which utilize clays as supports.

**Acknowledgment.** The authors would like to acknowledge F. W. Lytle, L. Chen, K. Pandya, L. Soderholm, M. A. Antonio, R. E. Winans, and M. Winterer for their technical expertise and helpful discussions. This work was performed under the auspices of the Division of Chemical Sciences, Office of Basic Energy Sciences, U.S. Department of Energy, under contract number W-31-109-ENG-38. Research at NSLS and SSRL is supported by the Department of Energy, Office of Basic Energy Sciences.

CM950330W